

Adsorption of Ideal Polymers on an Infinitely Ramified Fractal

F. D. A. Aarão Reis¹

Received September 29, 1997; final April 7, 1998

We study ideal polymer chains interacting attractively with the borders of the lacunas of an infinitely ramified fractal, the Sierpinski carpet. Ideal chains are simulated on finite stages of construction of this fractal at various temperatures. The mean-square displacement and the mean number of adsorbed monomers of N -step chains are estimated in these lattices, and extrapolations to the fractal limit (infinite lattice) consider the exact forms of finite-size corrections as previously predicted by the series expansion method. In the noninteracting case, a finite fraction of the monomers is adsorbed, and this fraction increases as the temperature decreases. However, there is evidence that the critical exponent ν which governs the growth of the chains varies with the temperature in a non-monotonic way. At high temperatures ν increases with decreasing temperature, and thus the chains are more stretched than in the noninteracting case. At an intermediate temperature, ν starts to decrease and is still positive at very low temperatures, when the chains grow along the borders of several lacunas, occasionally crossing the bulk between them.

KEY WORDS: Polymer adsorption; fractals; numerical simulations.

I. INTRODUCTION

The adsorption of polymers on attractive surfaces is a problem of great practical importance and has been studied for a long time.^(1,2) Statistical models which consider linear polymers on a lattice interacting with a rigid wall succeeded in representing those systems. The general picture which emerged from those studies revealed that the polymer undergoes an adsorption-desorption transition. At low temperatures, the chain grows along the attractive wall with loops in the bulk, and a finite fraction of the

¹ Instituto de Física, Universidade Federal Fluminense, Campus da Praia Vermelha, 24210-340 Niterói RJ, Brazil.

monomers adsorbed. At a critical temperature the number of adsorbed monomers M scales as $M \sim N^\Phi$, where N is the number of monomers in the chain and Φ is a crossover exponent. At higher temperatures M is finite even for very long chains ($N \rightarrow \infty$).

Recently, the increasing interest in physical systems in disordered media motivated a large number of studies of polymers on fractal structures.^(3,4,5) The effect of adsorbing boundaries, fractal or not, is also very important in these systems.⁽⁶⁾ The adsorption-desorption transition was observed in studies of ideal chains⁽⁷⁾ and self-avoiding walks^(8,10) on various finitely ramified fractals, considering one-dimensional, plane and also fractal attractive walls. There are also some experiments with polymers in porous media, such as a recent work with polystyrene confined in Vycor.⁽¹¹⁾

In this work we study ideal polymer chains interacting attractively with the lacunas of an infinitely ramified fractal, the Sierpinski carpet (SC), whose construction is shown in Fig. 1. In this model, configurations where the polymer enters a lacuna are forbidden, and the statistical weight is larger for configurations where one or more monomers slip along the borders of lacunas. The main difference to the fractals previously studied^(7,10) is that, in the SC, the adsorbing walls are distributed through the whole structure, simulating a porous medium with attractive internal surfaces. Consequently, important changes in the behavior of the chains are expected. We will show that there is no adsorption-desorption transition in this system: in the non-interacting case (or infinite temperature), a finite fraction of the monomers is adsorbed, and in the interacting case this fraction increases as the temperature decreases. However, there is evidence that the exponent ν , which governs the growth of the chain ($\nu = 1/D_c$, where D_c is the dimension of the chain), varies with the temperature in a non-monotonic way.

The ideal chain is the simplest model of linear polymers,⁽¹⁾ neglecting self-avoiding effects. The problem is defined in the same ensemble of the

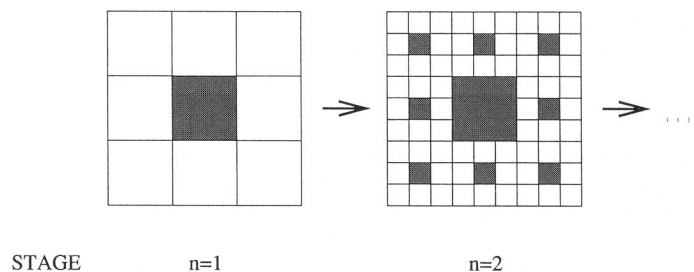


Fig. 1. Interactive construction of the Sierpinski carpet.

random walks, but the statistical weight of an N -step chain is x^N , where x is the step fugacity. Ideal chains and random walks are equivalent problems in Euclidean lattices, but are very different in fractal structures.⁽¹²⁾ If the chain interacts with a surface, the weight of an N -step chain with M steps along the surface is

$$W = x^N z^M \quad (1)$$

with

$$z = \exp(E/k_B T) \quad (2)$$

In Eq. (2), $-E$ is the energy of interaction ($E > 0$ in the attractive case) and T is the temperature.

Non-interacting ideal chains on the SC were previously studied using series expansions techniques.⁽¹³⁾ The exact number of chains and their mean-square displacements were obtained up to $N = 16$ in the fractal limit (stage $n \rightarrow \infty$; see Fig. 1). The series expansions technique⁽⁵⁾ is based on the calculation of the number of embeddings of the chains in a finite stage n of construction of the fractal, and a suitable extrapolation to $n \rightarrow \infty$. It is important to recall that approximation methods are necessary to solve such problems in infinitely ramified fractals, while in finitely ramified fractals it is often possible to construct exact recursion relations for the generating functions.^(7, 8, 9, 10)

It is very difficult to extend the series expansions technique to the interacting case because different embeddings in the same lattice may have different weights. On the other hand, simulations on finite stages of construction of the fractals give very accurate estimates of geometric properties for larger N , but they must be extrapolated to the fractal limit. In this work, the ideas of the extrapolation procedure developed by the series expansions technique will be used in the analysis of the results of numerical simulations on finite stages of the SC. We will obtain, in the fractal limit, very accurate estimates of the mean-square displacement $\langle R_N^2 \rangle$ and the mean number of adsorbed monomers $\langle M_N \rangle$, for relatively long chains ($N \approx 60$). Comparison with exact results for the non-interacting chains will prove the reliability of the method.

This work is organized as follows. In Section II we derive the expected dependence of $\langle R_N^2 \rangle_n$ and $\langle M_N \rangle_n$ on the stage n of the SC, based on the series expansions method. In Section III we discuss the simulations on finite stages of the SC and the procedure to estimate $\langle R_N^2 \rangle$ and $\langle M_N \rangle$ in the fractal limit, and compare these estimates with exact results up to $N = 16$ for the non-interacting ideal chains. In Section IV we present the

results for the ideal chains interacting with the borders of the lacunas of the SC. Section V contains our final conclusions.

II. RELATION BETWEEN GEOMETRIC QUANTITIES IN FINITE STAGES AND IN THE FRACTAL LIMIT

The series expansions technique was applied to study various statistical systems on regular fractals.^(5, 13, 14) The aim of this technique is to calculate exactly the number of embeddings of a connected graph in any stage n of the SC. As an example, in Fig. 2b we show two particular embeddings of a graph (a chain with three bonds, shown in Fig. 2a) in the second stage of the SC. It was proved that the total number of embeddings of a connected graph on stage n of the SC has the general form.

$$G(n) = A \cdot 8^n + B \cdot 3^n + C \quad (3)$$

where A , B and C are constants which depend on the graph and the fractal.⁽⁵⁾ Note that 8^n is the number of non-eliminated squares in stage n (see Fig. 1) and $L = 3^n$ is the length of the external border of stage n .

There is a minimum stage n_0 in which a graph can be embedded, and Eq. (3) is valid for $n \geq n_0$. Then, if a graph has N bonds, it is generally necessary that $N \leq 3^{n_0}$ to ensure that this graph can be embedded in stage n_0 (or $n > n_0$).

The mean square displacement $\langle R_N^2 \rangle_n$ and the mean number of adsorbed steps $\langle M_N \rangle_n$ of N -step ideal chains on stage n are

$$\langle R_N^2 \rangle_n = \frac{\sum_i G_i(n) R_i^2}{\sum_i G_i(n)} \quad (4a)$$

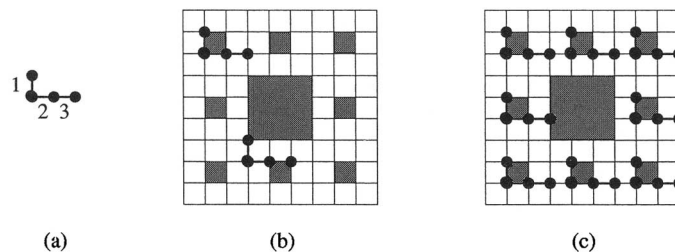


Fig. 2. (a) A graph with three bonds, labeled 1 to 3. (b) Examples of two embeddings of that graph on the second stage of the Sierpinski carpet. (c) All the embeddings of that graph whose bonds labeled 1 and 2 are absorbed at the border of a lacuna and whose bond labeled 3 is not absorbed.

and

$$\langle M_N \rangle_n = \frac{\sum_i \sum_{s_i} M(s_i) G_{s_i}(n)}{\sum_i G_i(n)} \tag{4b}$$

In Eqs. (4a) and (4b), i runs from 1 to 4^N (all the N -step chains) and $G_i(n)$ is the total number of embeddings of the chain i in stage n . R_i^2 (Eq. 4a) is the square of the end-to-end distance of chain i .

In Eq. (4b) we consider that different embeddings of the same graph have different numbers of adsorbed bonds. For instance, in Fig. 2b one embedding has two adsorbed bonds and the other has just one. If a graph has N bonds, each bond may be adsorbed or not, then there are 2^N possibilities of choosing the set of adsorbed bonds of a particular graph. In Eq. (4b), s_i runs from 1 to 2^N , representing all the possible sets of adsorbed bonds of graph i ; $G_{s_i}(n)$ is the number of embeddings of graph i in stage n with the set s_i actually adsorbed; $M(s_i)$ is the number of adsorbed bonds of this set. For instance, in Fig. 2c we show all the embeddings in stage $n=2$ of the graph shown in Fig. 2a, with the condition that the bonds labeled 1 and 2 are adsorbed and the bond labeled 3 is not adsorbed; then, $M(s_i) = 2$ and $G_{s_i}(2) = 8$ in this case.

In the derivation of Eq. (3), we considered that there are 8 reproductions of stage n at stage $n+1$, which obey the distribution of the squares in the generator. Then, the number of embeddings of a particular graph in stage $n+1$ is 8 times the number of embeddings in stage n , plus the number of embeddings crossing two or more reproductions of stage n at stage $n+1$.⁽⁵⁾ The same reasoning can be extended to the embeddings subject to the condition that the set of bonds s_i is adsorbed. Then $G_{s_i}(n)$ also has the general form of Eq. (3) (certainly, for some choices of the set s_i , $G_{s_i}(n) = 0$ for all n).

Thus we conclude that $\langle R_N^2 \rangle_N$ and $\langle M_N \rangle_n$ in Eqs. (4a) and (4b) have the general forms

$$\langle R_N^2 \rangle_n = \frac{A_1 \cdot 8^n + B_1 \cdot 3^n + C_1}{D_1 \cdot 8^n + E_1 \cdot 3^n + F_1} \tag{5a}$$

and

$$\langle M_N \rangle_n = \frac{A_2 \cdot 8^n + B_2 \cdot 3^n + C_2}{D_2 \cdot 8^n + E_2 \cdot 3^n + F_2} \tag{5b}$$

where $A_1, \dots, F_1, A_2, \dots, F_2$ are constants.

Eqs. (5a) and (5b) can be expanded as

$$\langle R_N^2 \rangle_n = \frac{A_1}{D_1} + a_1 \left(\frac{3}{8}\right)^n + b_1 \left(\frac{9}{64}\right)^n + c_1 \left(\frac{1}{8}\right)^n + \dots \quad (6a)$$

and

$$\langle M_N \rangle_n = \frac{A_2}{D_2} + a_2 \left(\frac{3}{8}\right)^n + b_2 \left(\frac{9}{64}\right)^n + c_2 \left(\frac{1}{8}\right)^n + \dots \quad (6b)$$

where a_1, b_1, \dots are constants related to A_1, \dots, F_1 , and a_2, b_2, \dots are constants related to A_2, \dots, F_2 . Eqs. (6a) and (6b) show the exact form of the finite-size corrections expected in this fractal. It is interesting to note that the leading corrections (second term in the right-hand sides) are proportional to L^{1-D_F} , where $L = 3^n$ is the length of the external border of stage n and

$$D_F = \frac{\log 8}{\log 3} \approx 1.8928 \quad (7)$$

is the fractal dimension of the SC. Then the factor L^{1-D_F} is simply the ratio of the length and the area of a lattice.

In the fractal ($n \rightarrow \infty$) we have

$$\langle R_N^2 \rangle = \frac{A_1}{D_1}, \quad \langle M_N \rangle = \frac{A_2}{D_2} \quad (8)$$

These results can be generalized to any regular fractal in a straightforward way.⁽⁵⁾

III. NUMERICAL SIMULATIONS AND EXTRAPOLATIONS TO THE FRACTAL LIMIT

The series expansions technique provides a systematic method to extrapolate quantities calculated in finite stages of a regular fractal, based on its rule of construction. This extrapolation method is sufficiently general to be used in the analysis of data obtained using any technique, exact or approximate.

Simulations of N -step ideal chains can be performed on various stages in which all these chains can be embedded. If the lengths of the lattices are $3^{n_0}, 3^{n_0+1}, \dots$, then it is necessary that $3^{n_0} \geq N$ to ensure that all the N -step chains can be embedded in all lattices (condition of validity of Eq. 3).

Eqs. (5a), (5b), (6a), (6b) show us the expected forms of the estimates $\langle R_N^2 \rangle_n$ and $\langle M_N \rangle_n$. If these estimates were obtained in six different stages

n ($n_0, \dots, n_0 + 5$), Eq. (5a) could be used to estimate the six constants A_1, \dots, F_1 , and Eq. (5b) used to estimate the six constants A_2, \dots, F_2 . From these constants we would get $\langle R_N^2 \rangle$ and $\langle M_N \rangle$ in Eq. (8).

However, in order to obtain estimates for relatively large N , and considering the condition $3^{n_0} \geq N$, we are able to use only three stages ($n = 4, n = 5$ and $n = 6$, with lengths 81, 243 and 729, respectively). Then we consider the three leading terms in the right-hand sides of Eqs. (6a) and (6b), use the estimates $\langle R_N^2 \rangle_n$ in the three stages above to obtain the coefficients $A_1/D_1, a_1$ and b_1 (Eq. 6a), and use the estimates $\langle M_N \rangle_n$ to obtain $A_2/D_2, a_2$ and b_2 (Eq. 6b).

The algorithm for simulating ideal chains is similar to the algorithm for simulating random walks,⁽¹⁵⁾ but requires a larger amount of data to produce accurate results. The initial site for each chain is randomly chosen over the lattice and N_{MAX} is its maximum number of steps. As we are interested in the conformational properties of the chains as functions of N (Eqs. 4a and 4b), and considering that the weight x^N (Eq. 1) is the same for all N -step chains, we do not need to take into account the weight x in the simulations. On the other hand, different chains with N steps have different statistical weights due to the different numbers of adsorbed bonds M (Eq. 1). Then, at each step, the probability to move to a neighboring site is proportional to z (Eq. 2b) if the step is along the border of a lacuna, and proportional to 1 if it is not.

We must also consider the effect of variable coordination numbers (from 2 to 4). Consider, for simplicity, the case $z = 1$ (no interaction). Two chains of $N - 1$ steps, labeled A and B, must be generated with equal probability p during the simulation. However, consider that the final site of chain A has y_A neighbors and the final site of chain B has y_B neighbors. Adding one bond to A or B, we produce an N -step chain. Then, any one of the N -step chains produced from A(B) will be generated with probability p/y_A (p/y_B). Thus, in order that all N -step chains have the same weight, the weight of a chain (used to compute the averages) must be multiplied by the coordination number of the original site of the step, at each step⁽¹⁶⁾ (y_A or y_B in the example above). Then the chains generated in the simulations will have statistical weights consistent with Eq. (2).

As the weights of the generated chains are distributed over various orders of magnitudes, a large number of chains are necessary to produce many statistically representative configurations. Then $\langle R_N^2 \rangle_n$ and $\langle M_N \rangle_n$ are averaged over 10^8 chains with $N_{\text{MAX}} = 81$ steps (in some cases, $N_{\text{MAX}} = 243$) on stages $n = 4, 5$ and 6.

In Table I we show $\langle R_N^2 \rangle$ for $N = 2$ to 16, obtained from results of simulations on stages $n = 4, 5$ and 6 and extrapolations considering the three leading terms in Eq. (6a). Results of two independent simulations

Table I. Estimates of Mean-Square Displacements $\langle R_N^2 \rangle$ of N -Step Noninteracting Ideal Chains on the SC^a

N	$\langle R_N^2 \rangle^{(a)}$	$\langle R_N^2 \rangle^{(b)}$	$\langle R_N^2 \rangle^{(c)}$	$\langle R_N^2 \rangle^{(d)}$
2	1.980951	1.979371	1.978104	1.975309
3	2.944840	2.944714	2.943169	2.940168
4	3.895467	3.894110	3.892373	3.890980
5	4.835754	4.839040	4.836802	4.832407
6	5.765094	5.771630	5.769373	5.763379
7	6.687493	6.701553	6.698501	6.686996
8	7.601847	7.609954	7.609055	7.602661
9	8.510022	8.525794	8.523750	8.512076
10	9.414640	9.424693	9.422962	9.414981
11	10.315014	10.314410	10.314629	10.312342
12	11.209340	11.199932	11.200905	11.204083
13	12.099884	12.090302	12.090749	12.090816
14	12.981129	12.963266	12.965617	12.972527
15	13.855963	13.843191	13.846809	13.849664
16	14.731540	14.731973	14.732207	14.722214

^a (a) and (b): simulations on stages $n = 4$, $n = 5$ and $n = 6$, extrapolations using three terms of Eq. (6a); (c): simulations on stages $n = 5$ and $n = 6$, extrapolations using two terms of Eq. (6a); (d): exact results (ref. 12).

(i.e., using different random number seeds in the simulations on each stage) are shown. The deviations from the exact results,⁽¹³⁾ shown in the last column, are always less than 0.3%. We also show $\langle R_N^2 \rangle$ obtained from simulations on stages $n = 5$ and $n = 6$ and extrapolations considering only the two leading terms of Eq. (6a) (i.e., only one finite-size correction term). The deviations are always less than 0.2%.

The data in Table I also show that the deviations of exact and approximate results do not increase systematically as N increases. This is essential to ensure the reliability of the results for larger N . However, the difference of $\langle R_N^2 \rangle_n$ in stage $n = 6$ and the exact $\langle R_N^2 \rangle$ increases with N , proving that the extrapolations to the fractal limit are absolutely necessary.

IV. RESULTS FOR IDEAL CHAINS INTERACTING WITH THE LACUNAS OF THE SC

Simulations at various reduced temperatures $t = k_B T/E$ between 0.3 and 6.0 were performed.

In Fig. 3 we show, at some temperatures, $m_N = \langle M_N \rangle / N$ versus $1/N$ up to $N_{\text{MAX}} = 81$, obtained from simulations in stages $n = 4$, $n = 5$ and $n = 6$ and extrapolations using three terms of Eq. (6b). We note that m_N rapidly

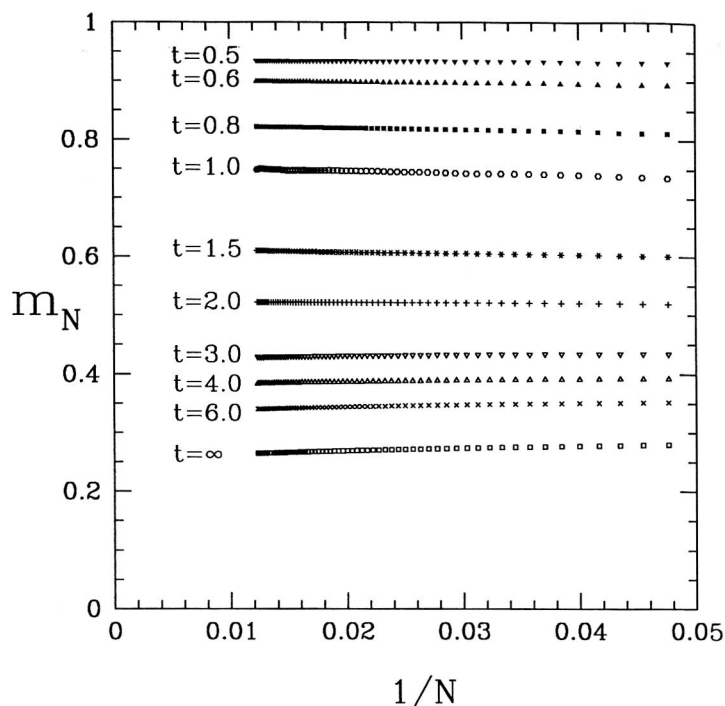


Fig. 3. Fraction of adsorbed monomers m_N of N -step ideal chains at various temperatures. The corresponding reduced temperatures $t = k_B T/E$ are indicated.

converges to their asymptotic values. Even for the non-interacting chains ($T = \infty$), m_N remains finite for large N , thus there is no desorption-adsorption transition when T decreases.

We estimate the fraction of adsorbed monomers for infinitely long chains, m_∞ , from least squares fits and parabolic fits of the data in Fig. 3 (for $N \geq 30$). Both fits give similar results. The fraction of non-adsorbed monomers $f_\infty = 1 - m_\infty$ is plotted in Fig. 4 as a function of inverse temperature. For sufficiently small temperatures we obtain

$$f_\infty \sim \exp(-C/T) \tag{9}$$

with $C \approx 1.3E/k_B$. The decrease of f_∞ with decreasing temperature is faster than the increase of the weight of the adsorbed monomers z (Eq. 2b), and the chain is almost completely adsorbed at low temperatures. However, since $f_\infty > 0$ and $\langle R_N^2 \rangle$ has a power law divergence at any finite temperature (this point is discussed below), the chain is never wrapped around a single lacuna.

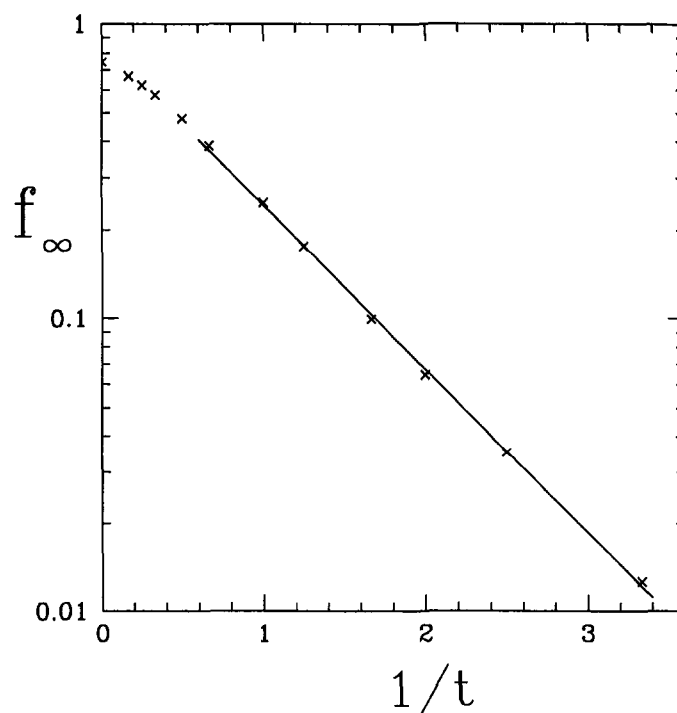


Fig. 4. Fraction of non-adsorbed monomers of infinitely long chains, f_∞ , versus inverse reduced temperature, $1/t = E/k_B T$. Data for $t=0.4$ and $t=0.3$, not shown in Fig. 3, are represented here. The straight line is a least squares fit of the last seven points.

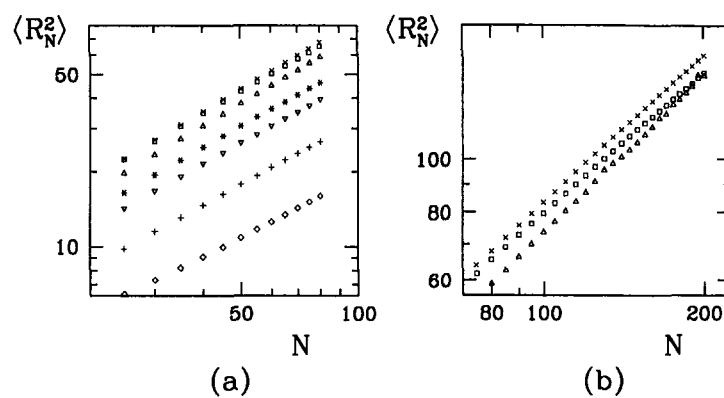


Fig. 5. Mean-square displacement $\langle R_N^2 \rangle$ of N -step ideal chains at various temperatures: $t = \infty$ (\square); $t = 6.0$ (\times); $t = 1.5$ (\triangle); $t = 1.0$ ($*$); $t = 0.8$ (∇); $t = 0.5$ ($+$); $t = 0.3$ (\diamond). Different extrapolations procedures were used to estimate $\langle R_N^2 \rangle$ in (a) and (b) (see text).

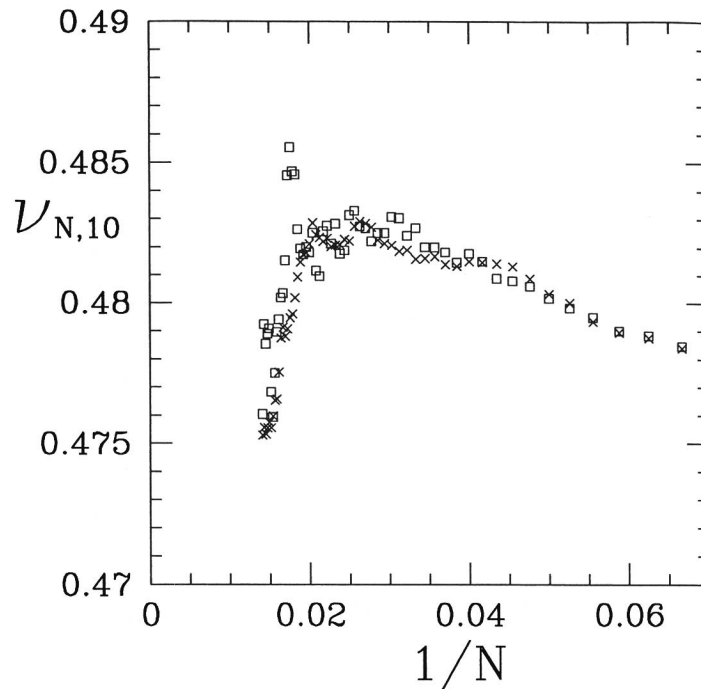


Fig. 6. Finite-size estimates $v_{N,10}$ (Eq. 11 with $i = 10$) for N -step ideal chains at $t = 3.0$ in two independent simulations.

In Fig. 5a we show $\langle R_N^2 \rangle$ versus N , for N up to 81, at various temperatures. These estimates are obtained with the same procedure as $\langle M_N \rangle$. Their errors are estimated from the scattering of the results of independent simulations, and are smaller than the size of the data point symbols. At high but finite temperatures, the chain grows faster than it grows at infinite temperature (non-interacting chain). It is confirmed by the results in Fig. 5b for N up to 200 ($t = \infty$, $t = 6.0$ and $t = 1.5$). They were obtained from simulations on stages $n = 5$ and $n = 6$ and extrapolations using only two terms in Eq. (6a). As the temperature decreases, the growth becomes slower.

At a fixed temperature and for large N the chains must behave as

$$\langle R_N^2 \rangle \sim N^{2\nu} \tag{10}$$

where ν is the critical exponent which measures the growth of the chain. It may be estimated from

$$v_{N,i} = \frac{\ln[\langle R_{N+i}^2 \rangle / \langle R_{N-i}^2 \rangle]}{\ln[(N+i)/(N-i)]} \tag{11}$$

When $N \rightarrow \infty$ we expect that $v_{N,i} \rightarrow v$ for finite i . In order to reduce the effect of statistical fluctuations in the data, we must consider large values of i in Eq. (11), but with $N \geq i$.

In order to analyse the effect of statistical errors on the estimates of $v_{N,i}$, we show in Fig. 6 results of two independent simulations at $t = 3.0$, using $i = 10$. For $N \lesssim 60$, the scatter of the data from different simulations is very small (the relative error is always less than 0.7%). For higher values of N , the deviations of different estimates is larger, and some oscillations appear. It may be related to strong finite-size effects on the estimates of $\langle R_N^2 \rangle_n$ in stage $n = 4$ ($L = 81$). Similar conclusions are obtained with other even values of i near $i = 10$ (odd values of i are not suitable for loose-packed lattices). Thus, our analysis of the exponent ν for the other temperatures will be based on results for $N \leq 60$.

In Fig. 7 we show $v_{N,i}$ for $i = 10$ at various temperatures. Note that we considered $v_{N,10}$ only up to $N = 50$, using $\langle R_N^2 \rangle$ up to $N = 60$ (Eq. 11). The estimated error bars are nearly $\Delta v = 0.001$ for all the data in Fig. 7; it corresponds to two or three times the size of the data point symbols.

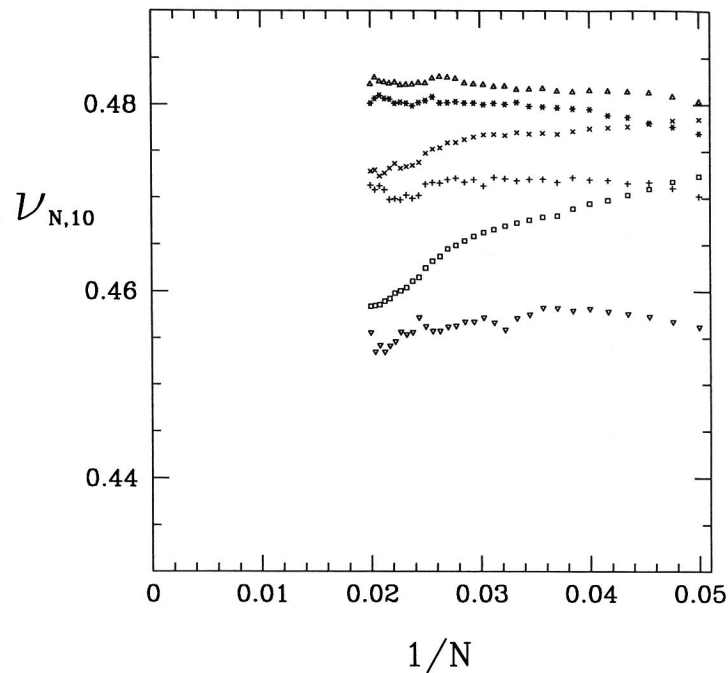


Fig. 7. Finite-size estimates $v_{N,10}$ (Eq. 11 with $i = 10$) for N -step ideal chains at various temperatures: $t = \infty$ (\square); $t = 6.0$ (\times); $t = 3.0$ (\triangle); $t = 2.0$ ($*$); $t = 1.5$ ($+$); $t = 1.1$ (∇).

$\nu_{N,10}$ is stable (at fixed temperature) until $t \approx 1.0$; below this temperature, the fluctuations are very large and the convergence is not clear as $N \rightarrow \infty$. Fig. 7 suggests that ν varies with the temperature, and that this variation is not monotonic. Up to $t \approx 3.0$, ν increases when the temperature decreases, i.e., the chain gets more stretched when adsorption is stronger. For $t \lesssim 3.0$, ν starts to decrease with temperature, but Fig. 5b indicates that a power law divergence of $\langle R_N^2 \rangle$ is still present at very low temperatures. In this regime, the chain grows along the borders of various lacunas (m_∞ is very near 1 at $t = 0.3$; see Fig. 4), and eventually crosses the bulk between adjacent lacunas.

The final estimates of ν are obtained from the convergence of $\nu_{N,10}$ (Fig. 7) at each temperature. For $t \lesssim 1.0$, we cannot obtain reliable estimates. An alternative analysis of our data was done using Padé approximants.⁽¹⁷⁾ Although the series are approximate, the convergence of the Padé approximants is surprisingly good for high temperatures. However, for $t \lesssim 1.5$ this method does not provide accurate estimates. In Fig. 8 we show the estimates

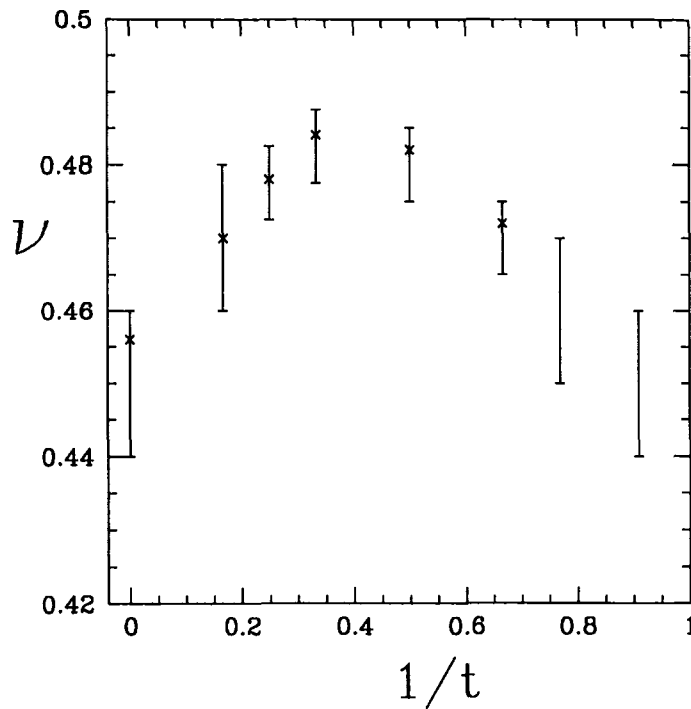


Fig. 8. Critical exponent ν (Eq. 10) versus inverse reduced temperature $1/t = E/k_B T$, obtained from $\nu_{N,10}$ (error bars) and from Padé approximants (\times , the central estimates).

of ν at various temperatures using both techniques: the error bars are obtained analysing $\nu_{N,10}$ and the points (\times) are central estimates obtained in a statistical analysis of Padé approximants ($25 \leq N \leq 80$).⁽¹⁸⁾ Both methods indicate the same non-monotonic dependence of ν on temperature.

As the fluctuations in $\langle R_N^2 \rangle$ increase rapidly with N and the estimates $\nu_{N,i}$ enlarge these fluctuations, the data for $N > 81$ do not give results better than the ones shown in Fig. 7. On the other hand, these estimates do not suggest any change of behavior for large N .

The idea of continuously varying exponents is unexpected, then it deserves some comments. The difference between the smaller and the greater estimates of ν is less than 10%, suggesting the possibility of temperature dependent amplitudes with the same asymptotic exponent. This scenario cannot be completely discarded, since we cannot discard the possibility of a change in the behavior of $\langle R_N^2 \rangle$ for much larger N . However, our analysis was performed with two extrapolation techniques generally used to avoid finite-size effects (on the length N), and the interpretation of variable ν is consistent with the properties of the model up to $N = 81$ extrapolated to $N \rightarrow \infty$. Moreover, temperature dependent critical exponents are found in related statistical problems on fractals,⁽¹⁹⁾ thus there is no special reason to reject this unusual property in a fractal system.

V. SUMMARY AND CONCLUSIONS

We have studied ideal chains interacting attractively with the lacunas of the SC. We developed a technique of calculation of geometric properties combining simulations on finite stages of the SC and extrapolations to the fractal limit based on results of the series expansions method. This technique gives very accurate estimates of the mean-square displacement $\langle R_N^2 \rangle$ and the mean number of adsorbed monomers $\langle M_N \rangle$ of N -step chains in the SC (infinite lattice). The estimates of $\langle R_N^2 \rangle$ for non-interacting chains are in good agreement with the exact results up to $N = 16$.⁽¹³⁾

At temperatures higher than $t \approx 1.0$ the chains are more stretched than at infinite temperature (non-interacting chains).

In order to understand this result, we must consider the “entropic trapping effect” of the highest coordination sites, which is characteristic of non-interacting ideal chains ($T \rightarrow \infty$) in several fractals.^(12, 13) In this case, the chains with the same length N have the same statistical weight x^N (Eq. 2, $T = \infty$). Then consider two sites, A and B , with coordinations $y_A > y_B$. The number of chains which cross site A is greater than the number of chains which cross site B , since there are more possibilities of steps from site A . As all the N -step chains have the same weight, a site of higher coordination will be crossed by a greater number of different chains than a site of low

coordination. In the SC this picture is supported by the estimate of the fraction of monomers in the borders of the lacunas $m_\infty \approx 0.26$ (see Fig. 3, $t = \infty$). This value is less than the fraction of sites in the borders of the lacunas, which is exactly $1/3$ in the SC. Thus it is clear the larger probability of the highest coordination sites (the bulk) being crossed by the ideal chains.

When the temperature decreases and the attraction to the lacunas appears, there is a larger statistical weight for steps along the border of lacunas. Then the probability of the low coordination sites being crossed by the chains increases. It happens as if the chain had got a larger portion of the lattice to grow (without a "preference" for the bulk), and the expected consequence is a faster growth. It is consistent with the increase of ν for large but finite t . The greatest estimate $\nu \approx 0.48$ is very close to the estimate for the random walks $\nu_w = 0.476 \pm 0.006$,⁽¹⁵⁾ and there is no entropic trapping effect in that problem. This is another result supporting the interpretation that the attraction to the lacunas compensates the entropic trapping to the high coordination sites. As t decreases, the probability of the low coordination sites being crossed by the chains increases, which is associated to the slower growth at $t \sim 2.0$.

At low temperatures ($t \lesssim 1.0$) the growth is slower, but still with a power-law divergence of $\langle R_N^2 \rangle$. The chain grows along the borders of various lacunas, and the fraction of nonadsorbed chains decays very rapidly (Eq. 9). Thus there are small jumps between adjacent lacunas instead of loops in the bulk. This is possible because lacunas of all sizes are spread on the whole lattice.

Although a continuous variation of critical exponents with the temperature is not expected in similar models in Euclidean lattices, it is important to recall that it may not be the case in fractals. For example, self-avoiding walks with curvature energy have temperature (or energy) dependent critical exponents in some fractals.⁽¹⁹⁾

We conclude that, although there is no adsorption-desorption transition in this model, there are interesting phenomena associated with the growth of the chain at various temperature ranges. In experiments with polymers on highly disordered media, we suggest the investigation of effects such as the non-monotonic variation of the growth exponent with temperature. Further work considering other polymer models, such as the self-avoiding walk, in fractals with $2 < D_F < 3$, would also be interesting to make a connection with real systems.

ACKNOWLEDGMENTS

This work was partially supported by CNPq and FINEP (Brazilian agencies).

REFERENCES

1. P. G. de Gennes, *Scaling Concepts in Polymer Physics* (Cornell University Press, Ithaca, New York, 1979).
2. K. Binder and K. Kremer, in *Scaling Phenomena in Disordered Systems*, R. Pynn and A. Skjeltrop, eds. (Plenum, New York, 1985).
3. R. Rammal, G. Toulouse, and J. Vannimenus, *J. Physique* **45**:389 (1984).
4. S. Haylin and B. Avraham, *Adv. Phys.* **36**, 695 (1987).
5. F. D. A. Aarão Reis and R. Riera, *J. Stat. Phys.* **71**:453 (1993).
6. P. Pfeifer, in *Fractals in Physics*, L. Pietronero and E. Tosatti, eds. (Elsevier Science Publishers, 1986).
7. M. Knezevic and D. Knezevic, *Phys. Rev. E* **53**:2130 (1996).
8. V. Bubanja, M. Knezevic, and J. Vannimenus, *J. Stat. Phys.* **71**:1 (1993).
9. S. Elezovic-Hadzic, M. Knezevic, S. Milosevic, and I. Zivic, *J. Stat. Phys.* **83**:1241 (1996).
10. S. Milosevic, I. Zivic, and V. Miljkovic, *Phys. Rev. E* **55**:5671 (1997).
11. J. Lal, S. K. Sinha, and L. Auvray, *J. Phys. II France* **7**:1597 (1997).
12. A. Giacometti, A. Maritan, and H. Nakanishi, *J. Stat. Phys.* **75**:669 (1994).
13. F. D. A. Aarão Reis and R. Riera, *Physica A* **208**:322 (1994).
14. F. D. A. Aarão Reis and R. Riera, *Phys. Rev. E* **49**:2579 (1994).
15. F. D. A. Aarão Reis, *J. Phys. A* **28**:6277 (1995).
16. J. Batoulis and K. Kremer, *J. Phys. A* **21**:127 (1988).
17. G. A. Baker, *Essentials of Padé Approximants* (Academic Press, New York, 1975).
18. A. J. Guttmann, *J. Phys. A* **20**:1839 (1987).
19. A. Giacometti and A. Maritan, *J. Phys. A* **25**:2753 (1992).